VSI: AOS Thesis 2020

Determining the Tractional Forces on Vitreoretinal Interface Using a Computer Simulation Model in Abusive Head Trauma

DONNY W. SUH, HELEN H. SONG, HOZHABR MOZAFARI, AND WALLACE B. THORESON

- PURPOSE: Abusive head trauma (AHT) is the leading cause of infant death and long-term morbidity from injury. The ocular consequences of AHT are controversial, and the pathophysiology of retinal research findings is still not clearly understood. It has been postulated that vitreoretinal traction plays a major role in the retinal findings. A computer simulation model was developed to evaluate the vitreoretinal traction and determine whether the distribution of forces in different layers and locations of the retina can explain the patterns of retinal hemorrhage (RH) seen in AHT.
- DESIGN: Computer simulation model study.
- METHODS: A computer simulation model of the pediatric eye was developed to evaluate preretinal, intraretinal, and subretinal stresses during repetitive shaking. This model was also used to examine the forces applied to various segments along blood vessels.
- RESULTS: Calculated stress values from the computer simulation ranged from 3-16 kPa at the vitreoretinal interface through a cycle of shaking. Maximal stress was observed at the periphery of the retina, corresponding to areas of multiple vessel bifurcations, followed by the posterior pole of the retina. Stress values were similar throughout all 3 layers of the retina (preretinal, intraretinal, and subretinal layers).
- CONCLUSIONS: Ocular manifestations from AHT revealed unique retinal characteristics. The model predicted stress patterns consistent with the diffuse retinal hemorrhages (RH) typically found in the posterior pole and around the peripheral retina in AHT. This computer model demonstrated that similar stress forces were produced in different layers of the retina, consistent with the finding that retinal hemorrhages are often found in multiple layers of the retina. These data can help explain the RH patterns commonly found in AHT. (Am J Ophthalmol 2021;223:396–404. Published by Elsevier Inc.)

ABUSIVE HEAD TRAUMA (AHT) ENCOMPASSES A form of inflicted head trauma in infants usually younger than 2 years of age. With or without blunt head trauma, AHT produces characteristic injuries to the central nervous system, cervical skeleton, and eyes, especially when the victim is subjected to repetitive acceleration and deceleration.[1] AHT is the leading cause of infant mortality and long-term morbidity from injury. Its prevalence in the United States has been estimated to be 30 of 100,000 children under the age of 1 year old, resulting in as many as 3 to 4 deaths per day.[1-4] Ocular pathology, including retinal hemorrhages (RH), retinoschisis, retinal detachment, and/or vitreous hemorrhages, is observed in approximately 85% of victims of AHT.[5–7] In most of these children, RH demonstrate multifocal and multilayered involvement extending to the ora serrata, with possible macular retinoschisis and vitreous hemorrhage. Although the exact mechanism for RH is not known, one hypothesis suggests it may be due to vitreoretinal traction that occurs during repetitive acceleration-deceleration with or without blunt head impact. Other theories explore the possibility of increased intravascular pressure as the culprit behind vascular wall damage and hemorrhage, seen in Valsalva maneuvers or chest injuries.[5,8] The exact reason for the extensive nature of RH involving the macula, periphery, and all layers of the retina is still not fully understood.

Since Caffey[9] first described RH in 1946, various animal and dummy doll model studies have shown that translational or linear oscillatory movements combined with a centrifugal force from concurrent rotational movements can potentially produce RH without contact trauma.[10–12] During shaking, the vitreous may cause shearing forces to be applied to the retina at points of firm attachment, including the macula, retinal vessels,

TABLE 1. Established FEM to Study AHT in Recent Years				
FEM Components	Hans and Associates[38]	Rangarajan and Associates[39]	Nadarasa and Associates[40]	Saffioti[41]
Cornea	✔	×	✔	✔
Sclera	✔	✔	✔	✔
Vitreous	✔	✔	✔	✔
Aqueous	✔	×	✔	×
Ciliary body	✔	×	✔	×
Lens	✔	×	✔	✔
Retina	✔	✔	✔	✔
Choroid	✔	×	✔	×
Tendons	✔	×	✔	×
Fatty tissue	✔	✔	✔	×
Skin	✔	×	✔	×

✔ = component was incorporated into their finite element; × = component was not included in their finite element; AHT = abusive head trauma; FEM = finite element model.

peripheral retina, and ora serrata. The high frequency of hemorrhages at the vitreous base and the unique macular retinoschisis of AHT support this theory. Also, studies using optical coherence tomography have shown significant disruption of the retinal microarchitecture with multilayered tractional retinoschisis intricately associated with focal posterior vitreous separation, supporting the theory of vitreoretinal interface shearing forces and its substantial role in the generation of retinal hemorrhages.[13–15]

However, few human subject studies with infants have been performed to bridge the knowledge gap between findings from computerized prototypes and in vivo animal model studies.[16–21] Most of what is known is provided by autopsy data, by dummy or replica doll models, and by animal models that have been used to study the causes of objective ocular findings including RH quantification.[10,22–24] Autopsy data from child abuse homicide investigations combined with a thorough study of historical facts from the confessions of suspected perpetrators and statements from the witnesses have been helpful in better understand the pathophysiology of the ocular damage. However, some autopsy data from cases without confessions and witnesses are limited by the lack of historical knowledge and mechanisms associated with the abuse. In vivo animal models allow the application of predetermined forces when examining ocular findings, but data interpretation and extrapolation to humans is a major challenge due to significant differences in the eye anatomy, functional components within the eye, retinal vasculature structure, head size, and neck anatomy between human infants and the animal models.[25–32] Dummy doll models with similar anatomical shape and weight to infants are helpful in determining biomechanics as a function of angular and linear acceleration but are limited in terms of biofidelity, and therefore, fail to integrate the local behavior of complex eyeball tissue upon external forces such as shaking. Results of these combined studies advance our understanding of AHT, but a better understanding of the biomechanics and pathophysiology of RH is critical to fully understand the ocular manifestations of AHT.

Computer simulations using finite element (FE) analysis offer a valuable way to study AHT.[33] This approach is relatively inexpensive compared to other models and has become popular due to its ability to incorporate both external and internal parameters that retain maximum biofidelity of the eyeball in response to predicted tissue stresses and strains. With the FE model, the eye is divided into very small pieces, akin to a brick (solid element) or thin plate (shell element), with physiological properties and characteristics that are similar to an infant's eye. These elements aggregate to produce an approximate model of an eye that can be manipulated computationally with relative conformity. Nodes can be created where the elements join to create flection points, and stresses may be applied to both the elements and nodes to measure resulting forces. Components of the infant's eye, such as the unique hyperviscous vitreous and firmly attached retina, can be incorporated into an FE eye model.[34,35] Since 1999, a number of FE analysis models applicable to AHT or shaken baby syndrome have been developed to study the blunt impact following ocular trauma.[36–40] However, previously models assumed a homogenous, full-surface attachment between the retina and vitreous, ignoring stronger adhesive forces in particular structures including perivascular areas.

To better understand the mechanisms associated with AHT ocular manifestations, namely RH, the present authors developed a new FE analysis of the eye and orbit that could be exposed to virtual forces experienced during shaking. A previous study of the physiologically biomimetic infant dummy doll by shaking by a human adult was used to define the parameters of acceleration, deceleration, range of motion of the eye in space, frequency of

TABLE 2. Material Properties of the Eye Components

Component	Element Type	Type of Law	Density (kg/m³)	ν[a]	Material Parameters
Sclera	Brick	Mooney-Rivlin	1,243	0.49	A = 495
					B = −470.2
Retina	Brick	Elastic	1,000	0.49	E = 11 kPa
Vitreous	Brick	Viscoelastic	1,009		G_0 = 0.01 kPa
					G_∞ = 0.0003 kPa
					B = 14.26 s⁻¹
					k = 2e + 6 kPa

A = Mooney-Rivlin Constants; B = Frequency; E = Young's Modulus; G_0 = Instantaneous shear modulus; G_∞ = Long-term shear modulus; k = Bulk modulus.

[a]Gr. nu = 0.0003 kPa.

shaking, and velocity. This helped us to determine the compressive and tractional forces as well as the pressure applied to the retina and its vasculature by using this FE model for the first time. Previous models subjected the eye only to simple rotational or translational movements along a single axis in an arc pattern. This new model was expanded by simulating multidirectional movements of the dummy doll model in a Figure 8 pattern. Furthermore, we also examined the forces applied to different layers of the retina by dividing it into preretinal, intraretinal, and subretinal spaces by using different elements forechain. This allowed more precise forces to be applied to different sublayers of the retina and thus a better understanding of the impact of the injury throughout the full thickness of the retina. This allowed a correlation to the retinal hemorrhage patterns commonly seen in AHT related to violent shaking.

This study sought to advance understanding of the pathophysiological process of vitreoretinal traction by determining the forces generated during shaking of an infant by using the newly developed FE model. The authors hypothesized that a newly developed FE model could advance understanding of vitreoretinal traction in AHT by determining the forces on posterior ocular tissues during shaking of an infant.

METHODS

• COMPUTER SIMULATION: FINITE ELEMENT EYE MODEL: Identification of key components of FE model development began with a medical literature review of previous eye models used historically to study AHT (Table 1). The different models incorporated various elements of the eye. To focus on the vitreoretinal interface and determine the retinal findings of AHT, a streamlined model was developed that retained the sclera, vitreous, and retina but excluded the cornea, iris, lens, and anterior segment to reduce any confounding factors. Also, to analyze the AHT-related retinal findings in more detail, 3 thin layers
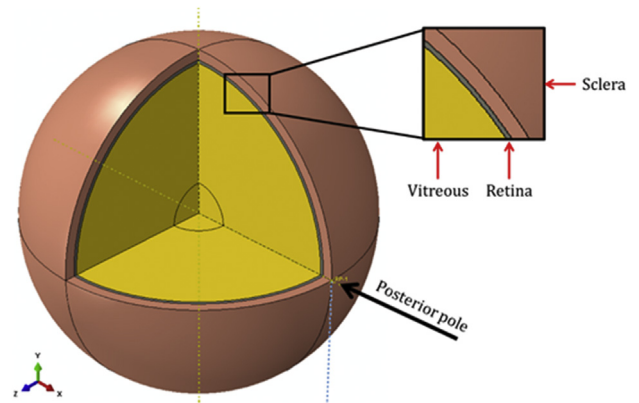

FIGURE 1. The eyeball components of the finite element model.

of elements were developed for the retina to represent preretinal, intraretinal, and subretinal layers, respectively. These layers were evaluated separately during shaking to isolate the impact of each individual layer. The key material properties of the model are listed in Table 2. Figure 1 illustrates the anatomy of our FE model.

Furthermore, to better simulate the location of vitreous attachments in vivo and, therefore, to better simulate the forces exerted at the retinal and vitreous interface during repetitive shaking, vitreoretinal attachment points were incorporated along all retinal vessels, the posterior pole, and the vitreous base of the eye globe. A standard fundus photograph was used to develop a map of the retinal vessels for incorporation into this model (Figure 2).

Afterwards, the FE eye model was created with 140,770 elements and 153,603 nodes. In other words, an eye was created using 300,000 small segments that could be individually analyzed in terms of eye position, forces exerted, and pressures applied when stress such as shaking was applied. Individual segments were analyzed simultaneously at 0.1-ms intervals throughout the shaking cycle.
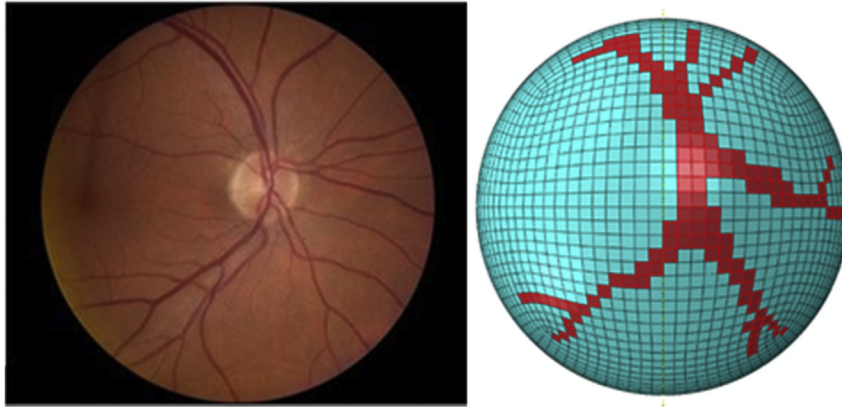
FIGURE 2. Retinal vessel attachment to the vitreous shown in a retinal image and the finite element model.

Once the FE model was designed, it was subjected to simulated shaking using values obtained from a biomimetic dummy model study. Yamazaki and associates[10] explored several modes of violent shaking using a dummy doll with an eyeball model to reproduce abusive events. In that study, an impersonating perpetrator with an accelerometer attached to one of his hands held the dummy doll facing himself while grasping the doll by the axillae. An additional accelerometer and pressure sensor were set on the eye and head of the doll. Using the FE model, shaking was simulated by using parameters similar to those measured by Yamazaki and associates[10] at a shaking frequency of 2.2 Hz (12.57 rad/s). Based on the results reported by Yamazaki and associates,[10] the maximum linear acceleration of 70 m/s^2 and a maximum angular acceleration during 1 cycle of 79.05 rad/s^2 were calculated. One full cycle of shaking was analyzed using the FE model. Data were analyzed on a continuous basis in a dynamic fashion to calculate the force and pressure applied to the elements and the nodes at any given point. Computational amplitude of shaking was condensed by 50% to reduce severe distortion of the elements that were noted on the FE element on a full scale. This may underestimate the stress calculated from this FE model during shaking. A reference point of shaking was coupled with the specified region on the outer surface of the sclera which would be consistent with perpetuator's elbow position and specifically at the location of the foveal region, in order to apply translational and rotational movements.

RESULTS

FOR THE FE SIMULATIONS, A SHAKING FREQUENCY OF 2.2 HZ (12.57 rad/s) was used, which yielded a maximum linear acceleration of 70 m/s^2 and a maximum angular acceleration during one cycle of 79.05 rad/s^2.[10] From FE analysis of the simulated eye, the forces applied to different layers and re-

gions of the retina at any given point during shaking were determined (Figures 3 and 4).

The stress contours at different time points during one cycle of shaking are shown for the preretinal, intraretinal, and subretinal layers in Figure 3 and Video 1 (the video is available at *www.ajo.com*). This pseudocolor heat map illustrates the stresses attained as a function of time during one cycle of shaking with higher stress values shown as warmer colors. As expected from the exclusive vitreous attachment points along blood vessels, the finite element model predicted that the greatest stress was concentrated along blood vessels and their bifurcations, with significantly less stress in nonvascular regions. At the initial time point of 0.0363 seconds (Figure 3, top row), there was a relatively uniform distribution of stress along the attached vessels. In the preretinal layers, slightly higher stress hotspots are visible at vessel bifurcations in peripheral retina (Figure 3, arrows). Stress was measured in kilopascals. One kPa is a unit of pressure obtained by force divided by the area and would be a pressure produced by 10 g (a pencil) mass resting on a 1-cm^2 area. One atmosphere (atm) is equal to 101.3 kPa. The average stress along the vessels is 7 kPa and rises to approximately 9-10 kPa at the vessel bifurcations in the preretinal layer and 8-9 kPa in the subretinal layer. With increasing acceleration at 0.1454 s, a similar distribution of stresses was observed, but the average stress along the vessels rose to approximately 8 kPa, with even higher values at the bifurcations (Figure 3, arrows). At 0.1999 s, when acceleration was at maximal, the stress reached 11 kPa along the vessels and at the bifurcations in both retinal layers. The maximum stress was attained at the macula, the peripapillary area, and at the vessel bifurcations near the ora serrata. The overall average stress of the entire retina including the vascular and nonvascular regions was 3 kPa.

In order to examine stress variations through the thickness of the retina, a segment of the retina with multiple elements near a bifurcation was selected (Figure 4). This figure shows average stresses measured at different levels
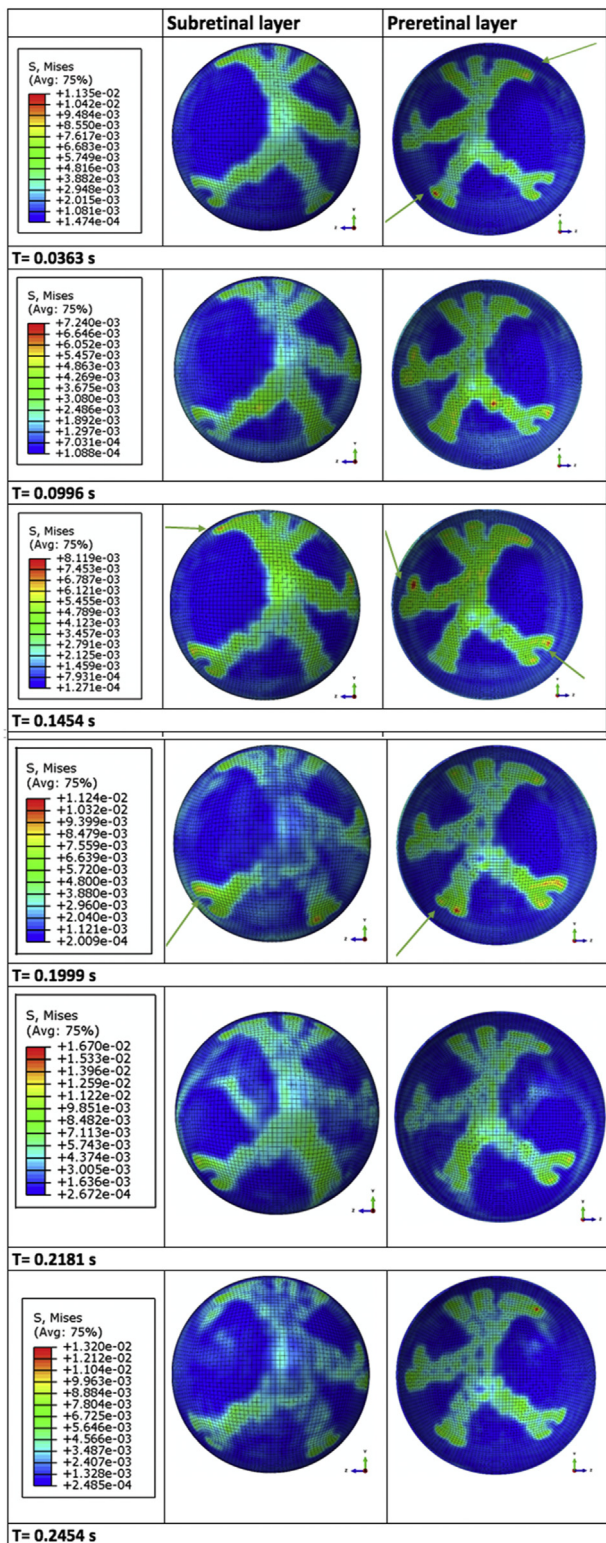
FIGURE 3. Force distribution on the retinal layers at various time frames illustrated by a pseudo-color heatmap at different time points during the cycle of acceleration resulting from shaking. Arrows designate regions of higher stress values. Arrows point to the areas of bifurcations.

across the entire retina. Although no statistical differences exist comparing preretinal to intraretinal and intraretinal to subretinal layers, there is a statistically significant difference between preretinal and subretinal layers ($P = .0015$), on average, 5.7 kPa compared to 4.4 kPa, respectively. The changes in stress values as a function of time during the one cycle of shaking also showed little difference among the different layers with no statistical differences (Figure 5).

DISCUSSION

RESULTS OF THE COMPUTER MODEL SHOW THAT SHAKING an eye at a frequency as low as 2.2 cycles per second can produce significant stress levels of 7 to 10 kPa along the retinal vessels. Coats and associates[20] studied the vitreoretinal adhesion in the equator and posterior pole in human eyes from donors ranging in age from 30 to 79 years old and in sheep eyes from premature, neonatal, young lamb, and young adult sheep. Their study found that the retinal peel force in donor eyes from young adults 30 to 39 years of age (7.24 ± 4.13 [millinewton] mN) was similar to that of immature and young sheep eyes (7.60 ± 3.06 mN).[42] Their results did not include the exact area of force applied, so conversion to kPa pressure units could not be done. If the area of the force applied to peel was 1 mm × 1 mm, the pressure would be approximately 7 kPa. Based on those results, mechanical failure of retinal tissue may occur in human infant eyes if stress levels exceed vitreoretinal adhesion.

With measured stress pressure values climbing to 10 kPa in the FE model at certain areas of vitreoretinal adhesions throughout the retina, this may exceed the vitreoretinal adhesion force. With multiple repetition of shaking and increased frequency, stress values may increase even farther. Also, there may be some degree of tissue fatigue that may lower the force needed to result in mechanical failure of retinal tissue from vitreous, resulting in acute separation of these 2 structures at or near the vessels.

A diagnosis of AHT requires agreement among an immense team of professionals from different medical disciplines and includes extensive radiological and laboratory investigations. Furthermore, a diagnosis has clinical, legal, and social implications for those involved.[43] With several cases usually proceeding to severe morbidity and mortality, the importance of recognizing clinical signs of abuse, especially ocular manifestations, is paramount. A false negative diagnosis that allows the child to return to the perpetrator can have a potentially fatal consequence. Although the Medical Justice Project of Northwestern University was the first to correlate geographical locations with reported cases of AHT, as many as 30% of AHT cases in the country may go unreported.[1–4,44] However, it is equally important
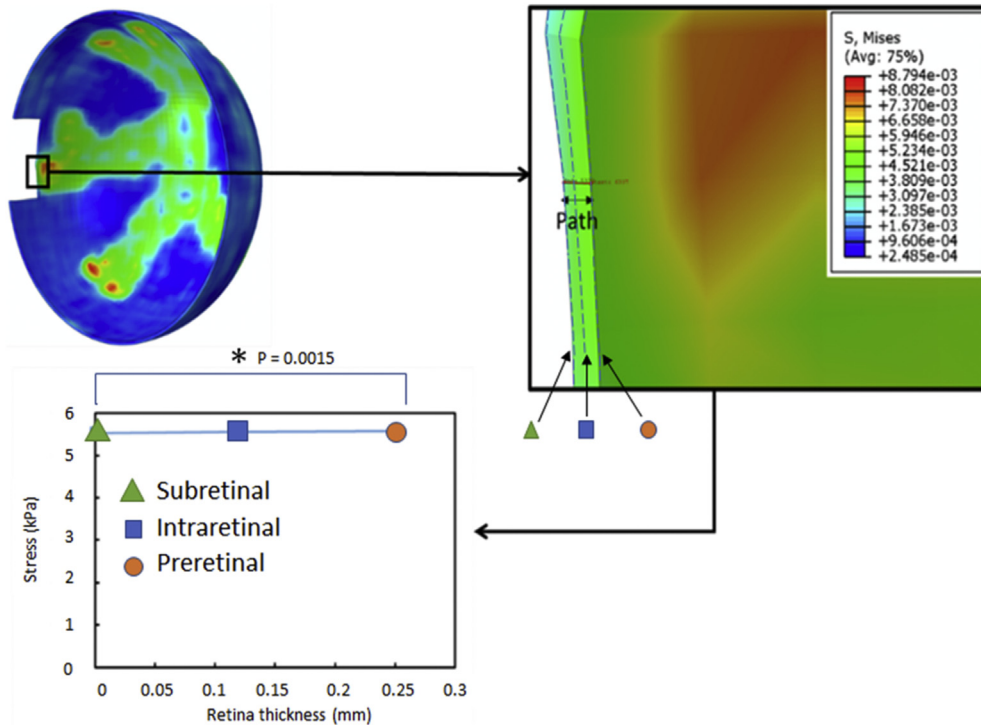
FIGURE 4. Stress variation through the thickness of the retina. The graph plots the average stresses measuredacross the entire retina at 3 different levels.

to rule out all potential differential diagnoses to ensure implications of abuse are not involved in unwarranted cases.[45,46] False positive cases can result in irreparable damage to the family's social dynamic.

For this new model, a frequency of shaking at 2.2 Hz was chosen. This frequency represents the average value of transducer-measured shaking performed by experimenters shaking a doll.[10] In that earlier study, the perpetrator shook the dummy doll with whole arms and synchronized the movement of the doll's body with that of its head. The horizontal displacement of the eyeball was maximal, exceeding 40 cm. Other studies have suggested that the frequency experienced by the head of a newborn during abusive shaking may be as high as 4 Hz.[45,47,48] However, the more conservative number of 2.2 Hz was chosen, which was more representative of an actual perpetrator shaking for our computer simulation model.

At a frequency of approximately 2.2 Hz, the head of an infant with a supple neck would travel a greater linear and angular distance. Even at that modest frequency, the forces exerted at the vitreoretinal surface could exceed 10 kPa based on the present FE analysis. This force may be sufficient to result in mechanical failure of retinal tissue due to stress. This may result in splitting of the retinal layers or retinoschisis or detachment of the vitreous from the retinal vessels, which may result in hemorrhage as a result

of compromise in the vascular lining and structure. Findings could be compatible by multiple optical coherence tomography studies revealing significant disruption of the retinal microarchitecture with multilayered tractional retinoschisis associated with posterior vitreous separation supporting a substantial role for the vitreoretinal interface in generating retinal hemorrhages.

In the present FE model, vessel bifurcations were subjected to greater stress than other areas of the retina, possibly due to the thin vascular wall in the peripheral retina and greater vessel surface area involved in vitreoretinal adhesions. Furthermore, as consecutive divisions of the branching vessels occurred, each generation of vessels became thinner and weaker as they grew into the periphery.[49] This may explain the diffuse RH patterns commonly found in the peripheral retina near the ora serrata of AHT, as these peripheral vessels with a greater number of bifurcations would receive a greater vitreoretinal stress force.

The current FE model revealed that the stress experienced by preretinal, intraretinal, and subretinal layers is similar in all three 3. Previous computer simulation models considered the retinal layer as a single spherical shell and did not examine how the stress was transmitted through the entire thickness of the retina. Also, previous models did not study the dynamic interaction between the vitreous and retina as the stress is transmitted throughout the
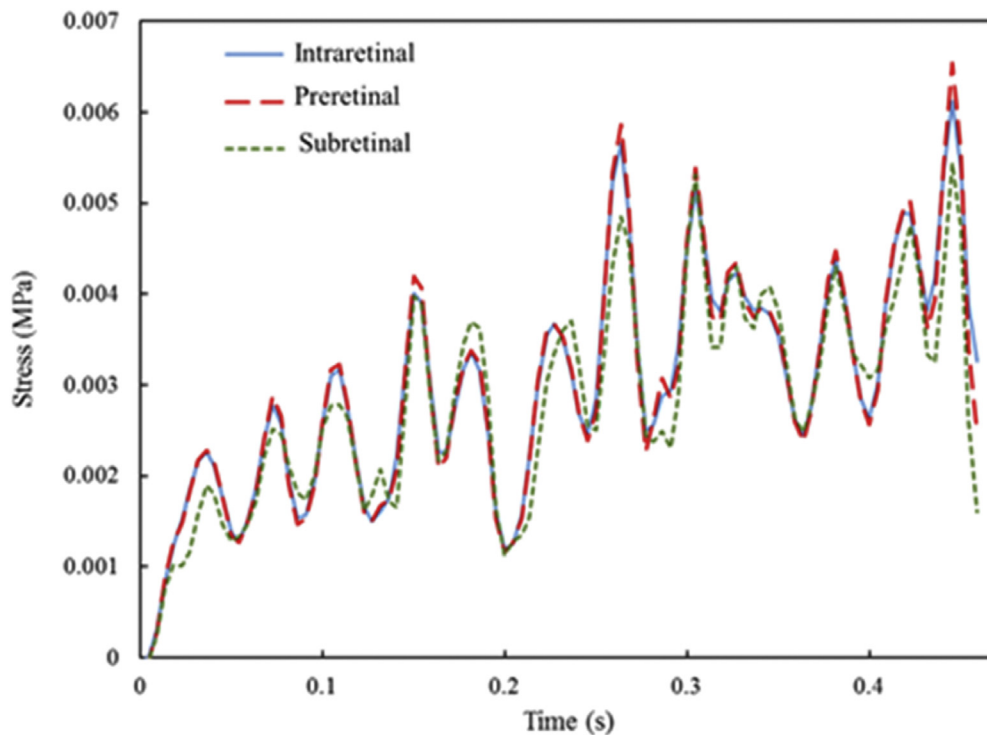
FIGURE 5. Time points of stress at the location of attached vessels for 3 layers of the retina. Theoscillations from simulated events result from back and forth movement of viscous structure of the vitreous.

retina.[38,39] We used 3 separate layers of solid elements throughout the entire retina to capture stresses in each sublayer. When the head is shaken, the eyeball experiences a significant displacement which induces shear and normal stress on the inner retinal layer by the relatively heavy vitreous.[10] The current FE model was able to analyze each layer of the retina separately, preretinal, intraretinal, and subretinal, as the force was transmitted during displacement of the eye. When shaking began, the highest stress value was experienced by the preretinal layer, whereas the lowest value was initially recorded at the subretinal layer. This is reflected by the statistical significance in stress between the preretinal and subretinal layers, comparatively and also may explain why preretinal hemorrhages are more frequently seen in AHT.[50] However, once the maximal speed was achieved, the disparities in stress levels among the 3 layers became statistically insignificant (when comparing preretinal to intraretinal layers and comparing intraretinal to subretinal layers, discretely), and the stress forces were transmitted equally throughout the entire thickness of the retina. Further studies are needed to provide mechanical properties, as the present model likely oversimplifies the nuances of each retinal layer. These studies will need to include detaching these thin layers and performing tension tests in order to differentiate them objectively to better understand the pathophysiology of retinoschisis and retinal detachment in AHT.

In contrast to our model predictions for shaking, in cases of increased intracranial pressure with cerebral edema or compressive subdural hematoma, increases in retinal venous pressure and axoplasmic transport interference of ganglion cell layers can result in peripapillary hemorrhages localized to the posterior pole with mostly intraretinal hemorrhages.[46,50–57] RH in AHT cases commonly show multilayered and diffuse RH involving the peripheral retina in addition to the macular area.[58–60], Suh and associates showed that infants delivered vaginally without complication may present with RH up to 50% of the cases, but most of these cases have only preretinal and intraretinal hemorrhages in the posterior pole with no signs of retinoschisis and vitreous hemorrhage that can be associated with vitreoretinal separation.[50,51] Furthermore, most of these RHs resolved within a few weeks, although a few isolated cases lasted up to 3 months of age.[50,51] The present FE model may shed light on pathophysiology of the RH patterns and differentiating findings in AHT from other causes.

In conclusion, this study describes development of a new FE analysis model that quantifies the distribution of forces at the vitreoretinal interface during shaking of AHT. This model advances the understanding of the pathophysiological process of vitreoretinal traction leading to mechanical failure during forcible shaking of the eyes. If the force generated during shaking is greater than the force needed

to maintain vitreoretinal adhesion, it may lead to retinal and vitreous separation acutely and breakdown of the blood vessel wall lining resulting in unique patterns of RHs. Ocular manifestations from AHT reveal unique retinal characteristics. The present FE model predicted stress patterns consistent with the diffuse RH typically found in the posterior pole and around the peripheral retina in AHT. This model also showed that similar stress forces are produced in different layers of the retina at maximal speed, consistent with the finding that retinal hemorrhages are often found in multiple layers of the retina and the retinoschisis in AHT. Thus, our results suggest that diffuse RH involving the periphery near the vessel bifurcations associated with multilayer retinal involvement would be suggestive of significant force applied to the retina that may led to mechanical failure. This information can be very useful for deciding whether to pursue the extensive and careful medical and social history investigation of circumstances surrounding a traumatic event.

REFERENCES

1. Hedlund GL. Subdural hemorrhage in abusive head trauma: imaging challenges and controversies. *J Am Osteopath Coll Radiol* 2012;1:23–30.

2. Binenbaum G, Mirza-George N, Christian CW, Forbes BJ. Odds of abuse associated with retinal hemorrhages in children suspected of child abuse. *J AAPOS* 2009;13:268–272.

3. Schroeder L. Hot spots-pinpointing shaken baby syndrome cases | Medill Justice Project. Available at: http://www.medilljusticeproject.org/2013/12/10/hot-spots/. Accessed December 10, 2013.

4. Keenan HT, Runyan DK, Marshall SW, Nocera MA, Merten DF. A population-based comparison of clinical and outcome characteristics of young children with serious inflicted and noninflicted traumatic brain injury. *Pediatrics* 2004;114:633–639.

5. Gabaeff SC. Challenging the pathophysiologic connection between subdural hematoma, retinal hemorrhage and shaken baby syndrome. *West J Emerg Med* 2011;12:144–158.

6. Kivlin JD, Simons KB, Lazoritz S, Ruttum MS. Shaken baby syndrome. *Ophthalmology* 2000;107:1246–1254.

7. Wright JN. CNS injuries in abusive head trauma. *AJR Am J Roentgenol* 2017;208:991–1001.

8. Morad Y, Kim YM, Armstrong DC, Huyer D, Mian M, Levin AV. Correlation between retinal abnormalities and intracranial abnormalities in the shaken baby syndrome. *Am J Ophthalmol* 2002;134:354–359.

9. Caffey J. The whiplash shaken infant syndrome: manual shaking by the extremities with whiplash-induced intracranial and intraocular bleedings, linked with residual permanent brain damage and mental retardation. *Pediatrics* 1974;54:396–403.

10. Yamazaki J, Yoshida M, Mizunuma H. Experimental analyses of the retinal and subretinal haemorrhages accompanied by shaken baby syndrome/abusive head trauma using a dummy doll. *Injury* 2014;45:1196–1206.

11. Bonfiglio A, Lagazzo A, Repetto R, Stocchino A. An experimental model of vitreous motion induced by eye rotations. *Eye Vis* 2015;2:10.

12. Caffey J. Multiple fractures in the long bones of infants suffering from chronic subdural hematoma. *Am J Roentgen Rad Ther* 1946;56:163–173.

13. Muni RH, Kohly RP, Sohn EH, Lee TC. Hand-held spectral domain optical coherence tomography finding in shaken-baby syndrome. *Retina* 2010;30(4 Suppl):S45–S50.

14. Sturm V, Landau K, Menke MN. Retinal morphologic features in shaken baby syndrome evaluated by optical coherence tomography. *Am J Ophthalmol* 2009;147:1102.

15. Sturm V, Landau K, Menke MN. Optical coherence tomography findings in shaken baby syndrome. *Am J Ophthalmol* 2008;146:363–368.

16. Donohoe M. Evidence-based medicine and shaken baby syndrome: part I: literature review, 1966-1998. *Am J Forensic Med Pathol* 2003;24:239–242.

17. Duhaime A-C, Gennarelli TA, Thibault LE, Bruce DA, Margulies SS, Wiser R. The shaken baby syndrome. A clinical, pathological, and biomechanical study. *J Neurosurg* 1987;66:409–415.

18. Duhaime AC, Alario AJ, Lewander WJ, et al. Head injury in very young children: mechanisms, injury types, and ophthalmologic findings in 100 hospitalized patients younger than 2 years of age. *Pediatrics* 1992;90:179–185.

19. Prange MT, Coats B, Duhaime A-C, Margulies SS. Anthropomorphic simulations of falls, shakes, and inflicted impacts in infants. *J Neurosurg* 2003;99:143–150.

20. Coats B, Binenbaum G, Peiffer RL, Forbes BJ, Margulies SS. Ocular hemorrhages in neonatal porcine eyes from single, rapid rotational events. *Invest Ophthalmol Vis Sci* 2010;51:4792–4797.

21. Kleinman PK. Diagnostic imaging of child abuse. Cambridge: Cambridge University Press; 2015.

22. Bandak FA. Shaken baby syndrome: a biomechanics analysis of injury mechanisms. *Forensic Sci Int* 2005;151:71–79.

23. Lantz PE, Stanton, CA. Postmortem detection and evaluation of retinal hemorrhages. Presented at the: AAFS Annual Meeting; February 2006; Seattle, Washington.

24. Wygnanski-Jaffe T, Levin AV, Shafiq A, et al. Postmortem orbital findings in shaken baby syndrome. *Am J Ophthalmol* 2006;142:233–240.

25. Prince JH. Anatomy and histology of the eye and orbit in domestic animals 1960. Springfield, IL: C. C. Thomas. Available at: https://catalog.hathitrust.org/Record/001516191. Accessed January 20, 2018.

26. Balazs EA, Denlinger JL. Aging and human visual function, vol.2. New York: Alan R Liss; 1982.

27. Luck JF, Nightingale RW, Loyd AM, et al. Tensile mechanical properties of the perinatal and pediatric PMHS osteoligamentous cervical spine. *Stapp Car Crash J* 2008;52:107–134.

28. Coats B, Binenbaum G, Smith C, et al. Cyclic head rotations produce modest brain injury in infant piglets. *J Neurotrauma* 2017;34:235–247.

29. Colter J, Williams A, Moran P, Coats B. Age-related changes in dynamic moduli of ovine vitreous. *J Mech Behav Biomed Mater* 2015;41:315–324.

30. Coats B, Saffioti JM. Age dependent and anisotropic material properties of immature porcine sclera, Vol 55607. ASME 2013 Summer Bioengineering Conference; 2013. V01AT05A015.

31. Anderson RWG, Sandoz B, Dutschke JK, et al. Biomechanical studies in an ovine model of non-accidental head injury. *J Biomech* 2014;47:2578–2583.

32. Finnie JW, Manavis J, Blumbergs PC. Diffuse neuronal perikaryal amyloid precursor protein immunoreactivity in an ovine model of non-accidental head injury (the shaken baby syndrome). *J Clin Neurosci* 2010;17:237–240.

33. Uchio E, Ohno S, Kudoh J, Aoki K, Kisielewicz LT. Simulation model of an eyeball based on finite element analysis on a supercomputer. *Br J Ophthalmol* 1999;83:1106–1111.

34. Rossi T, Boccassini B, Esposito L, et al. The pathogenesis of retinal damage in blunt eye trauma: finite element modeling. *Invest Ophthalmol Vis Sci* 2011;52:3994–4002.

35. Nickerson CS, Park J, Kornfield JA, Karageozian H. Rheological properties of the vitreous and the role of hyaluronic acid. *J Biomech* 2008;41:1840–1846.

36. Roth S, Raul J-S, Ludes B, Willinger R. Finite element analysis of impact and shaking inflicted to a child. *Int J Legal Med* 2007;121:223–228.

37. Raul J-S, Roth S, Ludes B, Willinger R. Influence of the benign enlargement of the subarachnoid space on the bridging veins strain during a shaking event: a finite element study. *Int J Legal Med* 2008;122:337–340.

38. Hans SA, Bawab SY, Woodhouse ML. A finite element infant eye model to investigate retinal forces in shaken baby syndrome. *Graefes Arch Clin Exp Ophthalmol* 2009;247:561–571.

39. Rangarajan N, Kamalakkannan SB, Hasija V, et al. Finite element model of ocular injury in abusive head trauma. *J Am Assoc Pediatr Ophthalmol Strabismus* 2009;13:364–369.

40. Nadarasa J, Deck C, Meyer F, Bourdet N, Raul J, Willinger R. Infant eye finite-element model for injury analysis. In: IRCOBI Conference Proceedings 2016. Available at: https://trid.trb.org/view/1426454. Accessed January 17, 2018.

41. Saffioti JM. Characterization of pediatric ocular material properties for implementation in finite element modeling 2014. https://collections.lib.utah.edu/dl_files/f7/0e/f70e353156fbc28372a89ec3ac90d2ecb1b8792d.pdf. Accessed August 2014.

42. Creveling CJ, Coats B. An innovative method for measuring adhesion at the vitreoretinal interface, Vol 1. National Harbor, MD: Curran Associates, Inc; 2016:1273–1274.

43. Narang SK, Estrada C, Greenberg S, Lindberg D. Acceptance of shaken baby syndrome and abusive head trauma as medical diagnoses. *J Pediatr* 2016;177:273–278.

44. Tuerkheimer D. The next innocence project: shaken baby syndrome and the criminal courts. *Washington University Law Review* 2009;87:1–58.

45. Jenny C, Bertocci G, Fukuda T, Rangarajan N, Shams T. Biomechanical response of the infant head to shaking—an experimental investigation. *J Neurotrauma* 2017;34:1579–1588.

46. Guthkelch AN. Infantile subdural haematoma and its relationship to whiplash injuries. *Br Med J* 1971;2:430–431.

47. Stern WE, Rand RW. Birth injuries to the spinal cord: a report of 2 cases and review of the literature. *Am J Obstet Gynecol* 1959;78:498–512.

48. Ommaya AK, Faas F, Yarnell P. Whiplash injury and brain damage: an experimental study. *JAMA* 1968;204:285–289.

49. Ponsioen TL, Hooymans JMM, Los LI. Remodelling of the human vitreous and vitreoretinal interface – A dynamic process. *Prog Retin Eye Res* 2010;29:580–595.

50. Kim SY, Suh DW. Comparison of the characteristics of retinal hemorrhages in abusive head trauma versus normal vaginal delivery. *J Am Assoc Pediatr Ophthalmol Strabismus* 2017;21:e24.

51. Morgan L, Jain S, Svec A, Svec C, Haney S, Allbery S, High R, Suh DW. Clinical comparison of ocular and systemic findings in diagnosed cases of abusive and non-abusive head trauma. *Clin Ophthalmol* 2018;12:1505–1510.

52. Shuman MJ, Hutchins KD. Severe retinal hemorrhages with retinoschisis in infants are not pathognomonic for abusive head trauma. *J Forensic Sci* 2017;62:807–811.

53. Vezina G. Assessment of the nature and age of subdural collections in nonaccidental head injury with CT and MRI. *Pediatr Radiol* 2009;39:586–590.

54. Emerson MV, Jakobs E, Green WR. Ocular autopsy and histopathologic features of child abuse. *Ophthalmology* 2007;114:1384–1394.

55. Reddy AR, Clarke M, Long VW. Unilateral retinal hemorrhages with subarachnoid hemorrhage in a 5-week-old infant: is this nonaccidental injury? *Eur J Ophthalmol* 2010;20:799–801.

56. Agrawal S, Peters MJ, Adams GGW, Pierce CM. Prevalence of retinal hemorrhages in critically ill children. *Pediatrics* 2012;129:e1388–e1396.

57. Greenwald MJ, Weiss A, Oesterle CS, Friendly DS. Traumatic retinoschisis in battered babies. *Ophthalmology* 1986;93:618–625.

58. Bhardwaj G, Jacobs MB, Martin FJ, et al. Photographic assessment of retinal hemorrhages in infant head injury: the Childhood Hemorrhagic Retinopathy Study. *J AAPOS* 2017;21:28–33.e2.

59. Yusuf IH, Barnes JK, Fung THM, Elston JS, Patel CK. Non-contact ultra-widefield retinal imaging of infants with suspected abusive head trauma. *Eye (Lond)* 2017;31:353–363.

60. Committee on Child Abuse and Neglect. Shaken baby syndrome: rotational cranial injuries—technical report. *Pediatrics* 2001;108:206–210.